# Auxin Activates the Plasma Membrane $H^+$-ATPase by Phosphorylation during Hypocotyl Elongation in Arabidopsis[1][W][OA]

**Koji Takahashi, Ken-ichiro Hayashi, and Toshinori Kinoshita***

Division of Biological Science, Graduate School of Science, Nagoya University, Nagoya, Aichi 464–8602, Japan (K.T., T.K.); and Department of Biochemistry, Okayama University of Science, Okayama 700–0005, Japan (K.-i.H.)

The phytohormone auxin is a major regulator of diverse aspects of plant growth and development. The ubiquitin-ligase complex $SCF^{TIR1/AFB}$ (for Skp1-Cul1-F-box protein), which includes the TRANSPORT INHIBITOR RESPONSE1/AUXIN SIGNALING F-BOX (TIR1/AFB) auxin receptor family, has recently been demonstrated to be critical for auxin-mediated transcriptional regulation. Early-phase auxin-induced hypocotyl elongation, on the other hand, has long been explained by the acid-growth theory, for which proton extrusion by the plasma membrane $H^+$-ATPase is a functional prerequisite. However, the mechanism by which auxin mediates $H^+$-ATPase activation has yet to be elucidated. Here, we present direct evidence for $H^+$-ATPase activation in etiolated hypocotyls of Arabidopsis (*Arabidopsis thaliana*) by auxin through phosphorylation of the penultimate threonine during early-phase hypocotyl elongation. Application of the natural auxin indole-3-acetic acid (IAA) to endogenous auxin-depleted hypocotyl sections induced phosphorylation of the penultimate threonine of the $H^+$-ATPase and increased $H^+$-ATPase activity without altering the amount of the enzyme. Changes in both the phosphorylation level of $H^+$-ATPase and IAA-induced elongation were similarly concentration dependent. Furthermore, IAA-induced $H^+$-ATPase phosphorylation occurred in a *tir1-1 afb2-3* double mutant, which is severely defective in auxin-mediated transcriptional regulation. In addition, $\alpha$-(phenylethyl-2-one)-IAA, the auxin antagonist specific for the nuclear auxin receptor TIR1/AFBs, had no effect on IAA-induced $H^+$-ATPase phosphorylation. These results suggest that the TIR1/AFB auxin receptor family is not involved in auxin-induced $H^+$-ATPase phosphorylation. Our results define the activation mechanism of $H^+$-ATPase by auxin during early-phase hypocotyl elongation; this is the long-sought-after mechanism that is central to the acid-growth theory.

The phytohormone auxin regulates diverse aspects of plant development, including tissue elongation, tropic growth, embryogenesis, apical dominance, lateral root initiation, and vascular differentiation (Teale et al., 2006). Proteins in the TRANSPORT INHIBITOR RESPONSE1/AUXIN SIGNALING F-BOX protein (TIR1/AFB) family have recently been demonstrated to function as nuclear receptors for auxin (Dharmasiri et al., 2005a; Kepinski and Leyser, 2005). The auxin signal transduction system operating via the E3 ubiquitin-ligase complex $SCF^{TIR1/AFB}$ (for Skp1-Cul1-F-box protein), which includes TIR1/AFBs, plays a critical role in many auxin-mediated responses through transcriptional regulation (Mockaitis and Estelle, 2008).

Auxin-induced elongation of plant organs, such as hypocotyls, coleoptiles, and roots, has been explained by the acid-growth theory since the 1970s (Rayle and Cleland, 1970; Hager et al., 1971; Moloney et al., 1981). The theory states that auxin enhances proton extrusion via the plasma membrane $H^+$-ATPase within several minutes. This process lowers the apoplastic pH, thereby promoting wall extension through the activation of wall-loosening proteins. In addition, the electrochemical potential gradient of protons across the plasma membrane that is created by the $H^+$-ATPase provides the driving force for $K^+$ uptake through inward-rectifying $K^+$ channels (Claussen et al., 1997; Philippar et al., 2006) and subsequent water uptake. These processes permit cell expansion, leading to elongation growth (Katou and Okamoto, 1992; Cosgrove, 2000; Hager, 2003). It has been reported that the early-phase auxin-induced hypocotyl elongation occurs in a quadruple mutant of the TIR1/AFB family proteins, *tir1-1 afb1-3 afb2-3 afb3-4* (Schenck et al., 2010), suggesting that transcriptional regulation is not essential for auxin-induced hypocotyl elongation. Thus, the plasma membrane $H^+$-ATPase plays a central role in auxin-induced elongation, but the mechanism by which auxin mediates the stimulation of the $H^+$-ATPase has

[1] This work was supported by the Ministry of Education, Culture, Sports, Science, and Technology, Japan (Grant-in-Aid nos. 21227001, 22119005, and 23370019 to T.K. and 23510285 to K.-i.H.) and the Advanced Low Carbon Technology Research and Development Program of the Japan Science and Technology Agency (grant to T.K.).

* Corresponding author; e-mail kinoshita@bio.nagoya-u.ac.jp.

The author responsible for distribution of materials integral to the findings presented in this article in accordance with the policy described in the Instructions for Authors (www.plantphysiol.org) is: Toshinori Kinoshita (kinoshita@bio.nagoya-u.ac.jp).

[W] The online version of this article contains Web-only data.

[OA] Open Access articles can be viewed online without a subscription.

www.plantphysiol.org/cgi/doi/10.1104/pp.112.196428

 

yet to be established (Hager et al., 1991; Frías et al., 1996; Jahn et al., 1996; Hager, 2003).

The plasma membrane H+-ATPase, a member of the superfamily of P-type ATPases, transports protons out of the cell in a process that is coupled to ATP hydrolysis and is important for intracellular pH homeostasis (Palmgren, 2001). The electrochemical gradient of protons across the plasma membrane regulates the membrane potential, which in turn affects channel activity and is utilized by secondary transporters; this process finally leads to a variety of physiological responses, including phloem loading, stomatal opening, solute uptake by the roots, and cell expansion. The phosphorylation of the penultimate amino acid Thr in the C terminus of the H+-ATPase and subsequent binding of a 14-3-3 protein to the phosphorylated C terminus is the major common mechanism by which the H+-ATPase is activated in plant cells (Sondergaard et al., 2004; Duby and Boutry, 2009). It should be noted that the H+-ATPase is phosphorylated at multiple sites in addition to the penultimate Thr (Fuglsang et al., 2007; Duby and Boutry, 2009; Rudashevskaya et al., 2012). In addition, protein kinase and phosphatase enzymes that directly regulate the phosphorylation level of the penultimate Thr of H+-ATPase have yet to be identified (Kinoshita and Hayashi, 2011). Many signals, including blue light, Suc, NaCl, phytohormones, and the fungal toxin fusicoccin (FC), regulate the phosphorylation level of the penultimate Thr in the C terminus of the H+-ATPase (Fuglsang et al., 1999; Kinoshita and Shimazaki, 1999, 2001; Svennelid et al., 1999; Kerkeb et al., 2002; Inoue et al., 2005; Niittylä et al., 2007; Chen et al., 2010). Phosphoproteomic analysis has shown that the phytohormone auxin induces phosphorylation of the penultimate Thr of the H+-ATPase isoform AHA1 in cultured Arabidopsis (*Arabidopsis thaliana*) cells (Chen et al., 2010). Therefore, we postulated that H+-ATPase is activated by this phosphorylation system during early-phase auxin-induced hypocotyl elongation.

In this study, we examined the molecular mechanism by which the plasma membrane H+-ATPase is activated during auxin-induced elongation in etiolated hypocotyls of Arabidopsis, showing that auxin induces elongation of the hypocotyl and activation of the H+-ATPase in a similar concentration-dependent manner. Moreover, we show that auxin-induced activation of the H+-ATPase via phosphorylation of the penultimate Thr in the C terminus occurs without the involvement of TIR1/AFBs.

## RESULTS

### Auxin-Induced Elongation of Arabidopsis Hypocotyls Requires H+-ATPase Activity

To investigate the mechanism of plasma membrane H+-ATPase activation during early-phase auxin-induced hypocotyl elongation, we established methods for the biochemical analysis of auxin-induced responses in Arabidopsis hypocotyls. Decapitated hypocotyl sections containing the elongating region were obtained from 3-d-old etiolated seedlings (Gendreau et al., 1997) and were stored on agar-solidified growth medium until a sufficient amount was gathered for analysis (Supplemental Fig. S1A). Although the hypocotyl sections continued to elongate on the growth medium in the presence of the exogenous natural auxin indole-3-acetic acid (IAA), hypocotyl elongation in the absence of IAA ceased within 30 min after excision (Supplemental Fig. S1B), as described previously (Christian and Lüthen, 2000). The transcript level of the auxin-inducible gene, *IAA1*, was also diminished in the hypocotyl sections 30 min after excision (Supplemental Fig. S1D). These results suggest that endogenous auxin in the hypocotyl sections becomes rapidly depleted after removal of the cotyledons.

When 10 $\mu$M IAA was applied to the auxin-depleted hypocotyl sections, elongation began after a short lag phase of around 10 min (Fig. 1A). Elongation reached a maximum rate of 8.8 $\mu$m min$^{-1}$ approximately 25 min after the addition of IAA; this rate was maintained for at least 60 min (Fig. 1C). The time course of the IAA-induced hypocotyl elongation was identical to that seen in a variety of previously studied plants (Evans, 1974; Schenck et al., 2010). Vanadate, an inhibitor of P-type ATPase, including the plasma membrane H+-ATPase (Kinoshita and Shimazaki, 1999), suppressed the IAA-induced elongation (Fig. 1A), suggesting that H+-ATPase activity is required for auxin-induced elongation.

### Auxin Induces Phosphorylation of the H+-ATPase in Hypocotyl Sections

The fungal toxin FC is known to enhance H+-ATPase activity through phosphorylation of the penultimate Thr as well as to induce elongation (Marre, 1979; Svennelid et al., 1999; Kinoshita and Shimazaki, 2001). Therefore, we examined the FC-induced hypocotyl elongation and H+-ATPase phosphorylation to confirm that our assay system was usable for analysis of the phosphorylation status of the H+-ATPase in response to auxin. The amount of H+-ATPase and the phosphorylation status of its penultimate Thr were detected by immunoblot analysis using anti-H+-ATPase and anti-pThr-947, respectively. These antibodies were raised against the catalytic domain of Arabidopsis H+-ATPase2 (AHA2) and the phosphorylated penultimate Thr-947 of AHA2 (described in detail in "Materials and Methods"; Hayashi et al., 2010). As shown in Supplemental Figure S2, FC-induced hypocotyl elongation and phosphorylation of H+-ATPase were detected, indicating that this assay system is suitable for analyzing H+-ATPase phosphorylation in Arabidopsis hypocotyls.

Next, we examined the phosphorylation status of the penultimate Thr of the H+-ATPase in hypocotyl sections in response to auxin. Exogenous IAA induced the phosphorylation of the H+-ATPase within 10 min. The phosphorylation level peaked 20 min after the

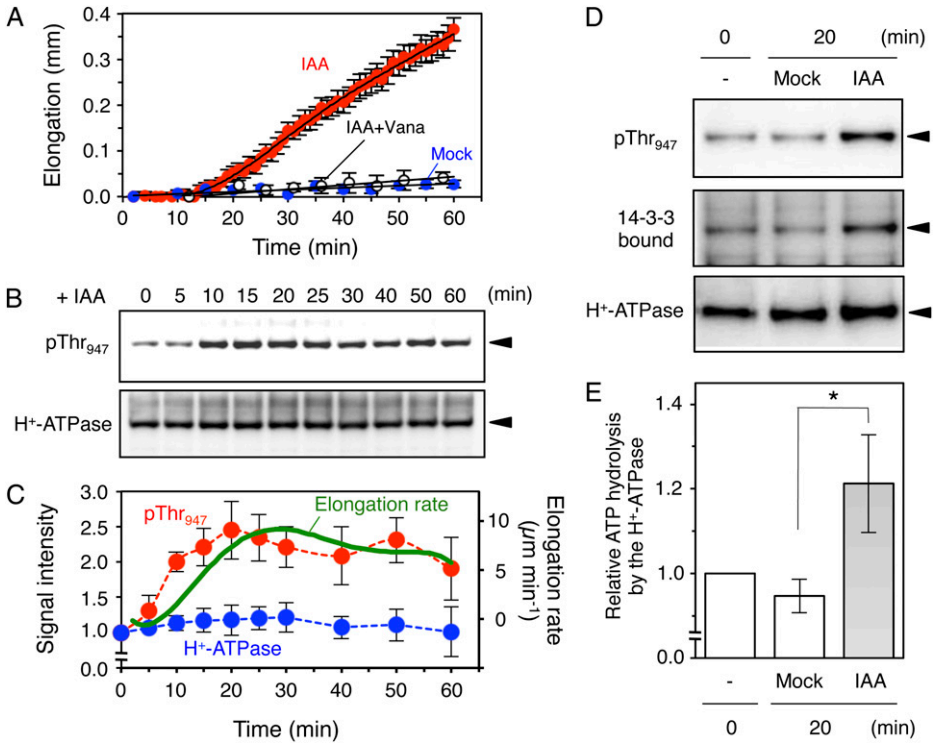


**Figure 1.** Auxin-induced hypocotyl elongation and activation of the plasma membrane $H^+$-ATPase via phosphorylation. A, Effect of auxin on hypocotyl elongation. Hypocotyl sections from 3-d-old etiolated Arabidopsis seedlings were treated with 10 $\mu$M IAA (IAA; red circles), 0.01% dimethyl sulfoxide (DMSO) as a vehicle (Mock; blue circles), and 10 $\mu$M IAA and 1 mM sodium orthovanadate (IAA+Vana; white circles) after depletion of endogenous auxin. The elongation of hypocotyl sections was measured after these treatments. Values are means ± SE; $n = 20$. Similar results were obtained in two additional independent assessments. B, Effect of auxin on $H^+$-ATPase phosphorylation in hypocotyl sections. Endogenous auxin-depleted hypocotyl sections were incubated with 10 $\mu$M IAA for the times indicated (min). The amounts of $H^+$-ATPase and the phosphorylation status of the penultimate Thr in the C terminus were determined by immunoblot analysis with anti-$H^+$-ATPase ($H^+$-ATPase) and anti-pThr-947 ($pThr_{947}$) antibodies, respectively. Arrowheads indicate the positions of the $H^+$-ATPase. C, Kinetics of IAA-induced elongation and IAA-induced $H^+$-ATPase phosphorylation. The plot shows the relative signal intensity of the immunoblot bands cross-reacted to anti-pThr-947 (red circles) and anti-$H^+$-ATPase (blue circles) antibodies. Values are means ± SD; $n = 3$. The elongation rate (green line) was calculated from the IAA-induced hypocotyl elongation depicted in A. The signal intensity is expressed relative to the intensity of the band signal at time zero. D, $H^+$-ATPase phosphorylation and binding of the 14-3-3 protein. Binding of the 14-3-3 protein was determined by protein-blot analysis using glutathione *S*-transferase-14-3-3 protein as a probe (14-3-3 bound). The rest of the procedure was as described for B. E, $H^+$-ATPase activity in hypocotyl sections. Vanadate-sensitive ATP hydrolysis was measured by determining the inorganic phosphate released from ATP. Values are means ± SD; $n = 3$. * $P < 0.05$, results of paired Student's *t* tests. For D and E, endogenous auxin-depleted hypocotyl sections were treated with 10 $\mu$M IAA (IAA) or 0.01% DMSO (Mock) for the times indicated.

addition of IAA and was maintained at this level for at least 60 min (Fig. 1, B and C). Phosphorylation of the $H^+$-ATPase preceded an increase in the hypocotyl elongation rate by about 5 min (Fig. 1C). Furthermore, IAA induced the binding of a 14-3-3 protein to the $H^+$-ATPase (Fig. 1D) and enhanced ATP hydrolysis by the plasma membrane $H^+$-ATPase in hypocotyl sections (Fig. 1E). In this study, we detected only 20% stimulation of ATP hydrolysis by auxin. It is most likely that the phosphorylated $H^+$-ATPase is subsequently dephosphorylated during the ATP hydrolysis assay, because the reaction mixture for this assay contains $Mg^{2+}$. Our previous work indicates that the phosphorylated $H^+$-ATPase is dephosphorylated in the presence of $Mg^{2+}$ in vitro (Hayashi et al., 2010).

We further examined the dose responses of $H^+$-ATPase phosphorylation and hypocotyl elongation to exogenous IAA. Both auxin responses changed dramatically between concentrations of 1 nM and 1 $\mu$M (Fig. 2, A and B); the responses were similarly concentration dependent and highly correlated ($r = 0.986$; Fig. 2C). The dose-response curve of IAA-induced hypocotyl elongation in Arabidopsis hypocotyls resembled those of other plant organs described previously (Cleland, 1972; Shinkle and Briggs, 1984). Taken together, these results indicate that auxin mediates the activation of the $H^+$-ATPase in hypocotyl sections via phosphorylation of its penultimate Thr, with subsequent binding of a 14-3-3 protein to the phosphorylated $H^+$-ATPase.

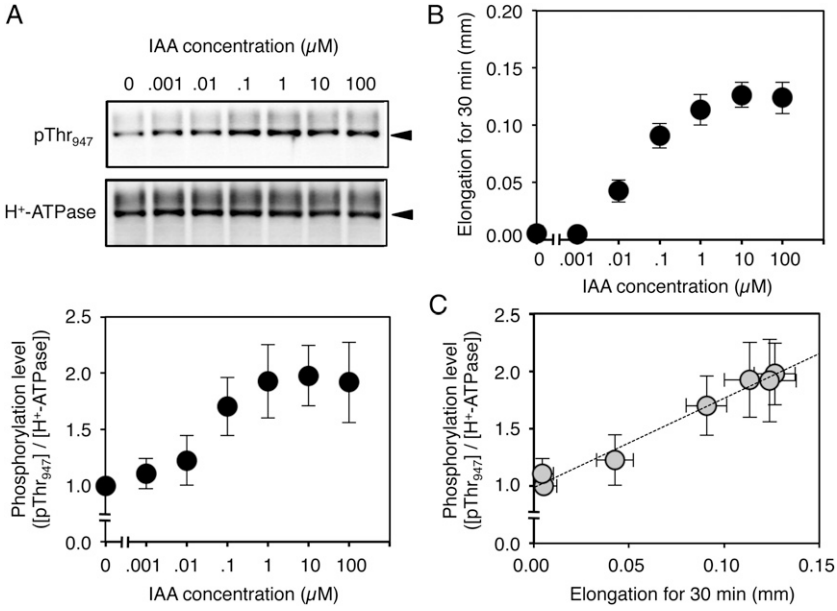


**Figure 2.** Dose responses of H+-ATPase phosphorylation and hypocotyl elongation to exogenous auxin application. A, Dose response of H+-ATPase phosphorylation to IAA. Endogenous auxin-depleted hypocotyl sections were incubated for 30 min in the presence of IAA at the concentrations indicated. The phosphorylation level of the H+-ATPase was quantified as the ratio of the signal intensity from the phosphorylated H+-ATPase to that from H+-ATPase and is expressed relative to the phosphorylation level of the hypocotyls that were not treated with auxin (graph at bottom). Values are means ± SD; $n = 3$ independent experiments. The rest of the procedure was as described in the legend to Figure 1B. B, Dose response of hypocotyl elongation to IAA. Hypocotyl elongation for 30-min periods was measured in the presence of IAA at the concentrations indicated. Values are means ± SE; $n = 20$. Similar results were obtained in two additional independent measurements. C, Correlation between the H+-ATPase phosphorylation level and IAA-induced hypocotyl elongation using the data in A and B ($r = 0.986$).

### Auxin Does Not Induce H+-ATPase Expression

As shown in Figure 1, the amount of H+-ATPase protein did not change for at least 60 min after IAA application. We analyzed the transcriptional level of H+-ATPase in the IAA-treated hypocotyls by quantitative reverse transcription (qRT)-PCR assays (Fig. 3). Relative transcriptional levels of *AHA1* and *AHA2*, which are the major H+-ATPase isogenes expressed in etiolated seedlings (Hayashi et al., 2010), were not changed by IAA treatment. In contrast, levels of the known auxin-inducible genes *KAT1* and *IAA1* (Abel et al., 1995; Philippar et al., 2004) increased more than 10-fold in response to IAA. Hence, an increase in the expression level of H+-ATPase is not required for early-phase auxin-induced hypocotyl elongation.

### Auxin Induces H+-ATPase Phosphorylation in *tir1-1 afb2-3* and *axr1-3* Mutant Plants

IAA-induced hypocotyl elongation was essentially unchanged, relative to the wild type, in both an auxin-receptor TIR1/AFB mutant, *tir afb*, and in the mutant *axr1-12*, the regulatory component of the $SCF^{TIR1/AFB}$ complex (Schenck et al., 2010), suggesting that auxin induces hypocotyl elongation in Arabidopsis without $SCF^{TIR1/AFB}$ signals. We then examined whether auxin induces H+-ATPase phosphorylation in the *tir1-1 afb2-3* double mutant (Savaldi-Goldstein et al., 2008) and the *axr1-3* mutant (Lincoln et al., 1990). IAA induced phosphorylation of the H+-ATPase in these mutants, and the phosphorylation level was increased to the same extent as in wild-type plants (Fig. 4A), suggesting that auxin increased the phosphorylation level of the penultimate Thr of the H+-ATPase without the involvement of TIR1/AFBs,

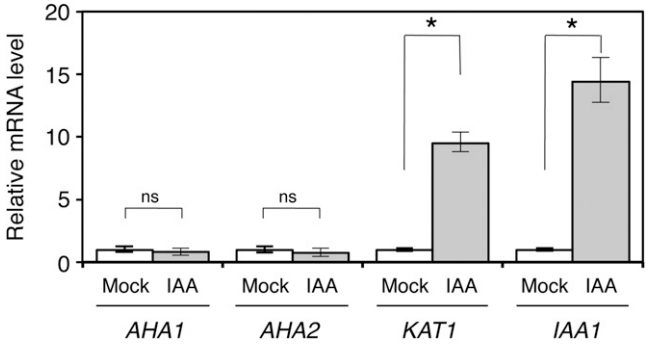


**Figure 3.** Effect of IAA on gene expression. qRT-PCR analysis of the H+-ATPase genes *AHA1* and *AHA2* and the known auxin-inducible genes *KAT1* and *IAA1* is shown. Total RNA was obtained from the hypocotyl sections 20 min after the application of 10 μM IAA (IAA) and 0.01% DMSO (Mock). Values are means ± SD; $n = 3$. * $P < 0.01$; ns, not significant at $P > 0.05$.

although the IAA-induced expression of *KAT1* and *IAA1*, and elongation in these mutants, were less than those in wild-type plants (Fig. 4B; Supplemental Fig. S4).

### Auxin-Induced Phosphorylation of the H$^+$-ATPase Is Not Affected by PEO-IAA and MG132

We next examined the effect of the auxin antagonist $\alpha$-(phenylethyl-2-one)-indole-3-acetic acid (PEO-IAA), which specifically binds to the auxin receptor TIR1/AFBs and blocks TIR1/AFB functions (Hayashi et al., 2008, 2012). Pretreatment with 100 $\mu$M PEO-IAA had no effect on the IAA-induced phosphorylation of the H$^+$-ATPase (Fig. 5A), although it suppressed the IAA-induced expression of *KAT1* and *IAA1* (Fig. 5C). In corroboration, pretreatment with 50 $\mu$M MG132, a proteasome inhibitor that inhibits ubiquitin-ligase complex SCF$^{TIR1/AFB}$-dependent responses (Dharmasiri et al., 2005b; Robert et al., 2010), also did not change the H$^+$-ATPase phosphorylation level but rather suppressed the IAA-induced expression of *KAT1* and *IAA1* (Fig. 6). Hence, phosphorylation of the H$^+$-ATPase is induced by auxin without involvement of the transcriptional system that contains the ubiquitin-ligase complex SCF$^{TIR1/AFB}$. It should be noted, however, that PEO-IAA and MG132 slightly suppressed IAA-induced hypocotyl elongation (Figs. 5B and 6B).

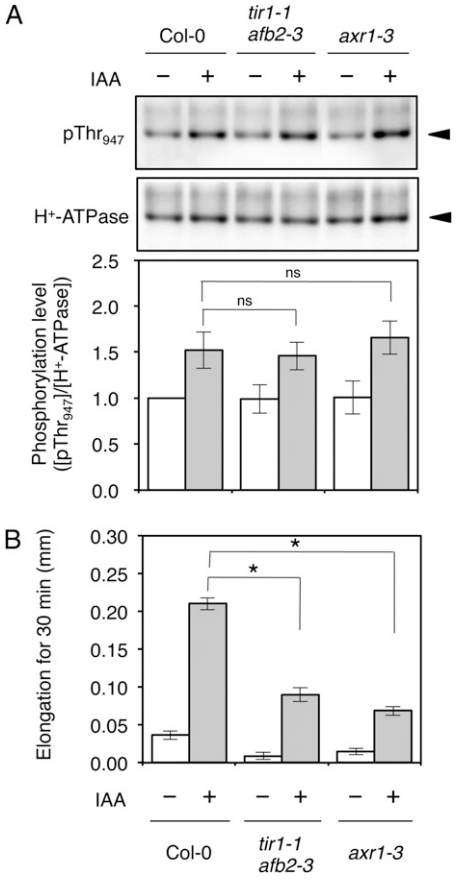


**Figure 4.** Auxin-induced H$^+$-ATPase phosphorylation and hypocotyl elongation in the *tir1-1 afb2-3* and *axr1-3* mutants. Hypocotyl sections depleted of endogenous auxin were incubated for 30 min in the absence (−) or the presence (+) of 10 $\mu$M IAA. A, IAA-induced H$^+$-ATPase phosphorylation. H$^+$-ATPase phosphorylation (pThr$_{947}$) levels and the amounts of H$^+$-ATPase (H$^+$-ATPase) were determined by immunoblot analysis using specific antibodies; the bottom plot depicts the phosphorylation level of the H$^+$-ATPase. Values are means ± SD; $n$ = 3 independent experiments. The rest of the procedure was performed as described in the legend to Figure 2A. B, Auxin-induced hypocotyl elongation. Hypocotyl elongation during periods of 30 min was measured. Values are means ± SE; $n$ = 15. Similar results were obtained in two additional independent measurements. * $P < 0.01$; ns, not significant at $P > 0.05$.

### Calyculin A and Okadaic Acid Inhibit Auxin-Induced H$^+$-ATPase Phosphorylation

Because calyculin A (CA)- and okadaic acid (OA)-sensitive protein phosphatases are most likely involved in the blue light-induced activation of H$^+$-ATPase in stomatal guard cells (Kinoshita and Shimazaki, 1997), we examined the effects of CA and OA, inhibitors of type 1/2A protein phosphatases, to determine the signaling pathway for auxin-induced H$^+$-ATPase phosphorylation. Interestingly, CA and OA completely inhibited the auxin-induced phosphorylation of the H$^+$-ATPase without affecting the quantity of the enzyme (Fig. 7A). Moreover, CA and OA inhibited the auxin-induced hypocotyl elongation (Fig. 7B). Thus, OA- and CA-sensitive protein phosphatases are very probably positive regulators in the signaling pathway between auxin perception and H$^+$-ATPase phosphorylation. These results suggest that phosphorylation of the penultimate Thr of the H$^+$-ATPase is required for auxin-induced hypocotyl elongation.

## DISCUSSION

### Auxin Activates the Plasma Membrane H$^+$-ATPase via Phosphorylation and Subsequently Induces Hypocotyl Elongation

Auxin-induced elongation of plant organs such as the stem, hypocotyl, and coleoptile is generally explained by the acid-growth theory, in which the plasma membrane H$^+$-ATPase plays a central role (Hager, 2003). However, the signaling pathway from auxin perception to H$^+$-ATPase activation has not been fully explored to date. In this study, we showed that IAA enhanced the phosphorylation level of the penultimate Thr of the plasma membrane H$^+$-ATPase in Arabidopsis hypocotyls within 10 min without altering the amount of the H$^+$-ATPase (Fig. 1, B and C). Then, a 14-3-3 protein bound to the phosphorylated H$^+$-ATPase, resulting in an elevation of the catalytic activity of the H$^+$-ATPase (Fig. 1, D and E). IAA induced phosphorylation of the H$^+$-ATPase approximately 5 min prior to hypocotyl elongation (Fig. 1C), and the P-type ATPase inhibitor,

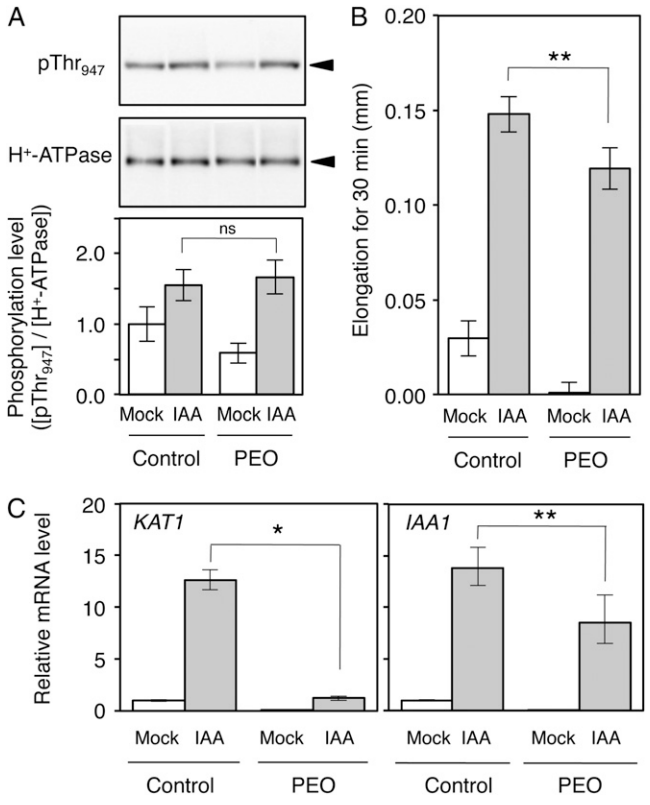


**Figure 5.** Effect of the auxin antagonist PEO-IAA on auxin responses. Hypocotyl sections depleted of endogenous auxin were treated with 100 $\mu$M PEO-IAA (PEO) or 0.1% DMSO (Control) for 60 min and then incubated for 30 min in the absence (Mock) or presence (IAA) of 10 $\mu$M IAA. A, Effect of PEO-IAA on H+-ATPase phosphorylation. Values are means ± SD; $n = 3$ independent experiments. Other details are provided in the legend to Figure 4A. B, Effect of PEO-IAA on auxin-induced hypocotyl elongation. Hypocotyl elongation was measured for 30-min periods. Values are means ± SE; $n = 15$. Similar results were obtained in two additional independent measurements. C, Effect of PEO-IAA on the expression of the auxin-inducible genes *KAT1* and *IAA1*. Relative expression levels of the genes were determined by qRT-PCR analysis. Values are means ± SD; $n = 3$. * $P < 0.01$; ** $P < 0.05$; ns, not significant at $P > 0.05$.

vanadate, suppressed the hypocotyl elongation. These observations indicate that auxin induces elongation via activation of the H+-ATPase by phosphorylation of the penultimate Thr. To our knowledge, this is the first experimental evidence to clarify the activation mechanism of the H+-ATPase during early-phase auxin-induced elongation.

A global quantitative analysis of the Arabidopsis phosphoproteome showed that the phosphorylation level of the penultimate Thr of AHA1 was elevated at 1, 3, and 6 h after application of 100 $\mu$M IAA in Arabidopsis suspension cells (Chen et al., 2010), indicating that the auxin-induced H+-ATPase phosphorylation might also occur in tissues other than the etiolated hypocotyls and that the phosphorylation is maintained for much longer than 60 min. In addition to the penultimate Thr, the H+-ATPase is phosphorylated at multiple other sites, especially in the C-terminal region (Fuglsang et al., 2007; Niittylä et al., 2007; Rudashevskaya et al., 2012). Further investigation is needed to examine whether auxin regulates the phosphorylation status of multiple sites in the plasma membrane H+-ATPase.

### Auxin-Induced H+-ATPase Phosphorylation without $SCF^{TIR1/AFB}$ Signals

Auxin enhanced the phosphorylation status of the H+-ATPase prior to hypocotyl elongation (Fig. 1). Recently, the auxin signal transduction system has been shown to be controlled by auxin perception by TIR1/AFBs and subsequent degradation of the auxin/IAA transcriptional repressors via the ubiquitin-proteasome pathway (Mockaitis and Estelle, 2008). However,

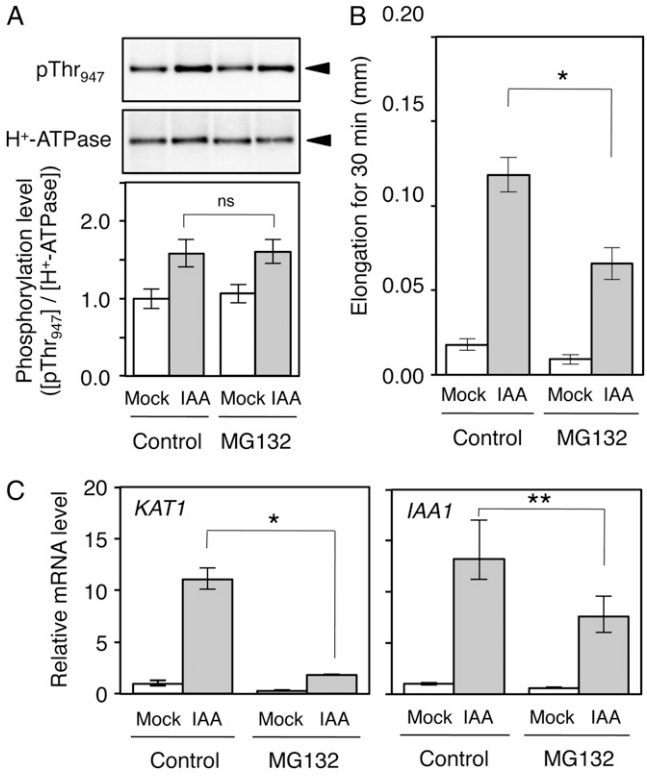


**Figure 6.** Effect of the proteasome inhibitor MG132 on auxin responses. Hypocotyl sections depleted of endogenous auxin were treated with 50 $\mu$M MG132 (MG132) or 0.1% DMSO (Control) for 60 min and then incubated for 30 min in the absence (Mock) or presence (IAA) of 10 $\mu$M IAA. A, Effect of MG132 on H+-ATPase phosphorylation. Details are provided in the legend to Figure 4A. Values are means ± SD; $n = 3$ independent experiments. B, Effect of MG132 on auxin-induced hypocotyl elongation. Hypocotyl elongation in 30-min periods was measured. Values are means ± SE; $n = 15$. Similar results were obtained in two additional independent measurements. C, Effect of MG132 on the expression of the auxin-inducible genes *KAT1* and *IAA1*. Relative expression levels of the genes were determined by qRT-PCR analysis. Values are means ± SD; $n = 3$. * $P < 0.01$; ** $P < 0.05$; ns, not significant at $P > 0.05$.

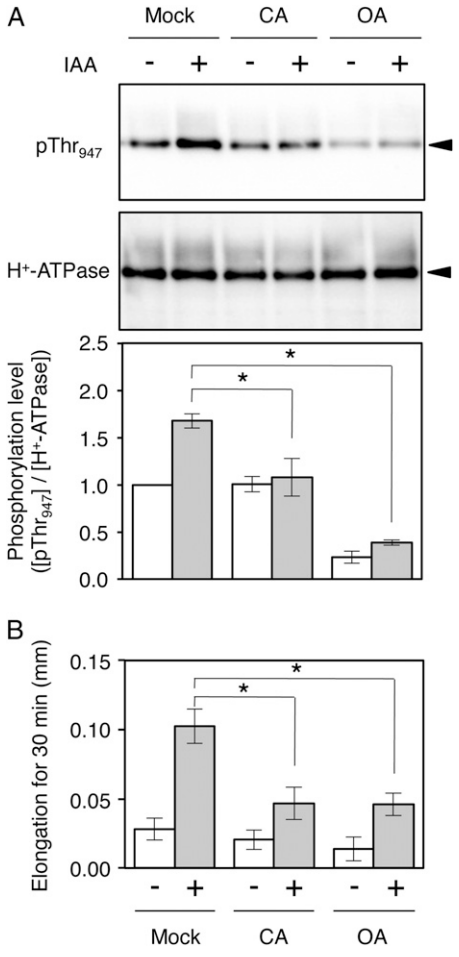


**Figure 7.** Inhibition of auxin-induced $H^+$-ATPase phosphorylation and hypocotyl elongation by protein phosphatase inhibitors. Hypocotyl sections depleted of endogenous auxin were preincubated with 1 $\mu$M CA (CA), 1 $\mu$M OA (OA), or 1% DMSO (Mock) for 60 min and then incubated for 30 min in the absence (−) or presence (+) of 10 $\mu$M IAA. A, Effect of protein phosphatase inhibitors on IAA-induced $H^+$-ATPase phosphorylation. Values are means ± SD; $n = 3$ independent experiments. * $P < 0.01$. The rest of the procedure was as described in the legend to Figure 4A. B, Effects of protein phosphatase inhibitors on IAA-induced hypocotyl elongation. Hypocotyl elongation was measured during 30-min periods. Values are means ± SE; $n = 15$. Similar results were obtained in two additional independent measurements. * $P < 0.01$.

auxin evokes hypocotyl elongation in the early phase, as demonstrated using a *tir afb* mutant and an *axr1* auxin-responsive mutant (Schenck et al., 2010), strongly suggesting that auxin induces elongation growth without involvement of the TIR1/AFBs. On the other hand, pharmacological analyses have revealed that inhibitors of protein and RNA synthesis rapidly inhibit auxin-induced elongation in coleoptiles (Cleland, 1971; Bates and Cleland, 1979; Edelmann and Schopfer, 1989), suggesting that de novo synthesis of the $H^+$-ATPase and/or the growth-regulating proteins such as expansins and $K^+$ channels are required for auxin-induced elongation. Thus, there has been controversy surrounding whether gene expression is involved in auxin-induced elongation growth.

The *tir1-1 afb2-3* and *axr1-3* mutants exhibited auxin-induced $H^+$-ATPase phosphorylation to the same extent as the wild type (Fig. 4A), and an antagonist of TIR1/AFBs, PEO-IAA, and the proteasome inhibitor MG132 had no effect on the auxin-induced $H^+$-ATPase phosphorylation (Figs. 5A and 6A). These genetic and pharmacological analyses indicate that auxin enhances the phosphorylation status of the $H^+$-ATPase penultimate Thr without the involvement of TIR1/AFBs. It should be noted that the involvement of other AFBs besides TIR1 and AFB2 in auxin-induced $H^+$-ATPase phosphorylation cannot be fully ruled out. On the other hand, the *tir1-1 afb2-3* double mutant and the *axr1-3* mutant exhibited less IAA-induced elongation than did the wild type (Fig. 4B; Supplemental Fig. S4). In addition, PEO-IAA and MG132 slightly suppressed IAA-induced hypocotyl elongation (Figs. 5B and 6B). These results suggest a partial involvement of TIR1/AFB-mediated expression of growth regulatory proteins that function downstream of the $H^+$-ATPase, such as KAT1, in auxin-induced hypocotyl elongation (Figs. 5 and 6; Supplemental Fig. S4).

### Auxin Signaling Pathway for $H^+$-ATPase Phosphorylation

The total protein and mRNA levels of $H^+$-ATPase were unchanged in response to auxin, suggesting that no increase in the expression of the $H^+$-ATPase was required for the early-phase auxin-induced elongation (Figs. 1 and 3). It has been reported that auxin induces exocytosis and the accumulation of the $H^+$-ATPase on the plasma membrane in maize (*Zea mays*) coleoptiles during elongation growth (Hager et al., 1991). In addition, auxin inhibits the trafficking of $H^+$-ATPase and PIN proteins from the plasma membrane to the endosomes (Paciorek et al., 2005) and the clathrin-dependent endocytosis mediated by AUXIN-BINDING PROTEIN1 (ABP1) in Arabidopsis roots (Robert et al., 2010). Taken together, these observations suggest that the intracellular localization of $H^+$-ATPase is regulated by auxin in the process of auxin-induced elongation. ABP1 has physiological affinities toward natural and synthetic auxin ligands (Hertel et al., 1972; Löbler and Klämbt, 1985) and has been shown to be involved in auxin-induced stimulation of the plasma membrane current by $H^+$-ATPase in the protoplasts of maize coleoptiles (Rück et al., 1993) and in the auxin-induced swelling of protoplasts from elongating *Pisum sativum* internodes (Yamagami et al., 2004). Thus, ABP1 probably functions in early-phase auxin-induced elongation (Perrot-Rechenmann, 2010). Further investigations are required to confirm whether ABP1 mediates the auxin-induced phosphorylation of $H^+$-ATPase by acting as an auxin receptor and to examine the intracellular localization of the $H^+$-ATPase in early-phase auxin-induced hypocotyl elongation. It has also been reported that a 57-kD auxin-binding protein of rice, $ABP_{57}$, activates

$H^+$-ATPase by direct interaction in response to auxin (Kim et al., 2001). Although there appear to be no genes homologous to the $ABP_{57}$ gene in Arabidopsis (Lee et al., 2009), it is possible that some receptor protein other than ABP1 functions in the auxin-induced $H^+$-ATPase phosphorylation of $H^+$-ATPase.

### Inhibitory Effects of CA and OA

Two inhibitors of type 1/2A protein phosphatases, CA and OA, completely inhibited the auxin-induced $H^+$-ATPase phosphorylation (Fig. 7), suggesting that an OA- and CA-sensitive protein phosphatase is a positive regulator in the signaling pathway between auxin perception and $H^+$-ATPase phosphorylation. This putative phosphatase is unlikely to be the one that directly dephosphorylates the $H^+$-ATPase, which is believed to be a type 2C protein phosphatase that is not inhibited by CA and OA (Hayashi et al., 2010).

Treatment of hypocotyl sections with OA decreased the basal level of $H^+$-ATPase and inhibited auxin-induced phosphorylation (Fig. 7A). Because type 2A protein phosphatases are more sensitive to OA than to CA (Ishihara et al., 1989), the much greater sensitivity of the $H^+$-ATPase phosphorylation level to OA than to CA suggests that a type 2A protein phosphatase may be involved in the signaling pathway between auxin perception and $H^+$-ATPase phosphorylation in the hypocotyl sections. This hypothesis, however, does not take into account the relative permeabilities of the inhibitors in the hypocotyl sections. In stomatal guard cells, it has been reported that the protein phosphatase sensitive to CA and OA functions downstream of the phototropins and upstream of the $H^+$-ATPase in the blue light signaling pathway (Kinoshita and Shimazaki, 1997; Hayashi et al., 2011), suggesting a possible common mechanism in blue light signaling and the auxin-induced phosphorylation of $H^+$-ATPase. In addition, CA has been reported to disturb membrane trafficking in lily (*Lilium longiflorum*) pollen tubes (Foissner et al., 2002; Hörmanseder et al., 2005). Taken together, these reports suggest that CA and OA might affect the intracellular localization of $H^+$-ATPase by endomembrane trafficking.

## CONCLUSION

The $H^+$-ATPases, which are ubiquitous in all plant cell types that have been investigated, provide the driving force for the uptake of numerous nutrients through coupling with organ-specific transporters; these enzymes are essential for cell growth and development (Palmgren, 2001). In elongating hypocotyls, the $H^+$-ATPase is mainly localized in epidermal and vascular tissues (Supplemental Fig. S5), and its activity in each tissue is thought to be enhanced by auxin (Katou and Okamoto, 1992). In this study, we have provided evidence that phosphorylation of the penultimate Thr of the $H^+$-ATPase activates the $H^+$-ATPase, which stimulates hypocotyl elongation. This chain of events occurs independently of the TIR1 and AFB2 auxin receptors.

## MATERIALS AND METHODS

### Plant Material and Auxin Treatment

The Arabidopsis (*Arabidopsis thaliana*) mutants *tir1-1* (CS3798), *afb2-3* (SALK_137151), and *axr1-3* (CS3075) from the Arabidopsis Biological Resource Center were all in the Columbia ecotype. Arabidopsis seedlings were grown on Murashige and Skoog plates in darkness for 3 d at 24°C. Hypocotyl sections of 4 mm (Supplemental Fig. S1A) were excised using a razor blade from etiolated seedlings and incubated on growth medium (10 mM KCl, 1 mM MES-KOH [pH 6.0], and 0.8% [w/v] agar) for 0.5 to 2.0 h in darkness to deplete endogenous auxin (Supplemental Fig. S1D). During the incubation, hypocotyl elongation ceased and the $H^+$-ATPase was dephosphorylated (Supplemental Fig. S1, B and C). We performed auxin treatments by transferring the preincubated hypocotyl sections to growth medium containing 10 $\mu$M IAA, except where otherwise noted. The hypocotyl sections were photographed with a digital camera (Supplemental Fig. S1E), and the length of the center line drawn on the hypocotyl section was measured using ImageJ software to estimate the elongation length (Supplemental Fig. S1F). The values reported here are averages from 15 to 20 hypocotyl sections. Experiments were repeated at least three times. Inhibitors were tested by incubating preincubated hypocotyl sections for 60 min on growth medium containing inhibitors before the auxin treatment. Because IAA-induced hypocotyl elongation and $H^+$-ATPase phosphorylation show variability between different batches of hypocotyl sections, the comparative experiment shown in each figure was carried out using hypocotyl sections from the same batch. All manipulations were carried out under dim red light.

### Determination of $H^+$-ATPase Phosphorylation Levels

The amount of plasma membrane $H^+$-ATPase and the phosphorylation level of its penultimate Thr in the hypocotyl sections were determined by immunoblot analysis using specific antibodies against the catalytic domain of AHA2 and phosphorylated Thr-947 in AHA2 (Hayashi et al., 2010). These antibodies recognize not only AHA2 but also other $H^+$-ATPase isoforms in Arabidopsis (Hayashi et al., 2011). Fifteen pieces of hypocotyl sections were collected into a 1.5-mL plastic tube and immediately frozen with liquid $N_2$. The frozen tissues were ground with a plastic pestle, followed by solubilization in 40 $\mu$L of SDS buffer (3% [w/v] SDS, 30 mM Tris-HCl [pH 8.0], 10 mM EDTA, 10 mM NaF, 30% [w/v] Suc, 0.012% [w/v] Coomassie Brilliant Blue, and 15% [v/v] 2-mercaptoethanol), and the homogenates were centrifuged at room temperature (10,000*g* for 5 min). Aliquots containing 10 or 20 $\mu$L of the supernatant were loaded onto 9% (w/v) acrylamide gels to analyze the amount of $H^+$-ATPase or the phosphorylated Thr, respectively. SDS-PAGE and immunoblot analysis were performed as described previously (Hayashi et al., 2010). A goat anti-rabbit IgG conjugated to horseradish peroxidase (Bio-Rad Laboratories) was used as a secondary antibody, and the chemiluminescence from the horseradish peroxidase reaction with a chemiluminescence substrate (Pierce) was detected using the Light Capture AE-2150 system (Atto). The chemiluminescent signal was quantified using ImageJ software. The differences in signal intensity corresponded to the amount of the cross-reacted proteins because the signal intensity was proportional to the amount of proteins loaded (Supplemental Fig. S3, A and B). The ratio of the signal intensity from the phosphorylated $H^+$-ATPase to that from the $H^+$-ATPase obtained from the same sample was constant (Supplemental Fig. S3C). Therefore, the phosphorylation level of the $H^+$-ATPase was quantified from the ratio and is expressed relative to the phosphorylation level of a control sample.

### Measurement of Vanadate-Sensitive ATPase Activity

ATP hydrolysis by the plasma membrane $H^+$-ATPase was measured in a vanadate-sensitive manner following the method of Kinoshita and Shimazaki (1999) with some modifications. Hypocotyl sections were homogenized in homogenization buffer (50 mM MOPS-KOH [pH 7.0], 2.5 mM EDTA, 100 mM NaCl, 1 mM dithiothreitol, 1 mM phenylmethylsulfonyl fluoride, 20 $\mu$M

leupeptin, and 0.025% Triton X-100) using a plastic pestle and strained through a 58-$\mu$m nylon mesh. The filtered homogenate was then mixed with an equal volume of reaction mixture (50 mM MOPS-KOH [pH 7.0], 0.2 M mannitol, 100 mM NaCl, 100 mM $KNO_3$, 2.5 mM EDTA, 20 mM $MgCl_2$, 10 $\mu$g $mL^{-1}$ oligomycin, 1 mM ammonium molybdate, 0.5 mM phenylmethylsulfonyl fluoride, and 10 $\mu$M leupeptin), with and without 100 $\mu$M sodium orthovanadate, for the measurement of ATPase activity. The reaction was initiated by adding 2 mM ATP and run for 30 min at 24°C.

## Real-Time qRT-PCR

Total RNA was isolated using the RNeasy Plant Kit (Qiagen); first-strand cDNA was synthesized with the PrimeScript II First Strand cDNA Synthesis Kit (TaKaRa). qRT-PCR was performed using the Power SYBR Green PCR Master Mix and the StepOne Real-Time PCR system (Applied Biosystems). For gene-specific amplifications of the *AHA1*, *AHA2*, *KAT1*, and *IAA1* transcripts, the following primer sets were used: for *AHA1*, 5′-GAACGTCCTGGGGCGC-3′ and 5′-GATACCCTTCACCTTTGCAAATGT-3′; for *AHA2*, 5′-TTGTTGA-ACGTCCTGGAGCA-3′ and 5′-AATTCC CAGTTGGCGTAAACC-3′; for *KAT1*, 5′-GGAGCAGTGGACTTCACTGTC-3′ and 5′-GCGATGTTCTGCT-TATCCGCAG-3′; and for *IAA1*, 5′-CACCGACCAACATCCAATCTCC-3′ and 5′-TGGACGGAGCTCCATATCTCC-3′. Relative quantification was performed using the comparative cycle threshold method, and the relative amount of PCR product amplified using the above primer sets was normalized to the *TUB2* gene fragment as an internal control amplified with the primers 5′-AAACTCACT-ACCCCCAGCTTTG-3′ and 5′-CACCAGACATAGTAGCAGAAATCAAGT-3′. The relative expression levels of the target genes were compared with the ratios in auxin-depleted hypocotyl sections.

## Immunohistochemical Detection of Plasma Membrane $H^+$-ATPase in Hypocotyls

Immunohistochemical detection was performed following previous methods (Paciorek et al., 2006; Hayashi et al., 2011) with modifications. Transverse sections (8 $\mu$m) of hypocotyl sections on microscope slides were heated in phosphate-buffered saline (137 mM NaCl, 8.1 mM $Na_2HPO_4$, 2.68 mM KCl, and 1.47 mM $KH_2PO_4$) for 1 min at 105°C for antigen retrieval. The sections were blocked in a blocking solution of 3% bovine serum albumin fraction V (Sigma) in phosphate-buffered saline for 1 h at room temperature and then incubated overnight at room temperature with anti-$H^+$-ATPase and preserum diluted 1:1,000 in blocking solution. After washing of the sections, they were incubated at room temperature for 3 h with goat anti-rabbit IgG conjugated to Alexa Fluor 488 (Invitrogen) diluted 1:1,000 in blocking solution. After washing, the transverse sections were observed with a fluorescence microscope (BX50; Olympus) and images were captured with a CCD camera system (Olympus DP72).

## Supplemental Data

The following materials are available in the online version of this article.

**Supplemental Figure S1**. Preparation of hypocotyl sections for analysis of auxin-induced responses.

**Supplemental Figure S2**. FC-induced hypocotyl elongation and $H^+$-ATPase phosphorylation.

**Supplemental Figure S3**. Detection of the plasma membrane $H^+$-ATPase and the phosphorylated $H^+$-ATPase in Arabidopsis hypocotyl sections.

**Supplemental Figure S4**. Auxin-induced hypocotyl elongation and gene expression in the *tir afb* and *axr1* mutants.

**Supplemental Figure S5**. Localization of the plasma membrane $H^+$-ATPase in etiolated Arabidopsis hypocotyls.

Received February 27, 2012; accepted April 2, 2012; published April 5, 2012.

## LITERATURE CITED

**Abel S, Nguyen MD, Theologis A** (1995) The *PS-IAA4/5*-like family of early auxin-inducible mRNAs in *Arabidopsis thaliana*. J Mol Biol **251:** 533–549

**Bates GW, Cleland RE** (1979) Protein synthesis and auxin-induced growth: inhibitor studies. Planta **145:** 437–442

**Chen Y, Hoehenwarter W, Weckwerth W** (2010) Comparative analysis of phytohormone-responsive phosphoproteins in *Arabidopsis thaliana* using $TiO_2$-phosphopeptide enrichment and mass accuracy precursor alignment. Plant J **63:** 1–17

**Christian M, Lüthen H** (2000) New methods to analyse auxin-induced growth. I. Classical auxinology goes *Arabidopsis*. Plant Growth Regul **32:** 107–114

**Claussen M, Lüthen H, Blatt M, Böttger M** (1997) Auxin-induced growth and its linkage to potassium channels. Planta **201:** 227–234

**Cleland R** (1971) Instability of the growth-limiting proteins of the Avena coleoptile and their pool size in relation to auxin. Planta **99:** 1–11

**Cleland R** (1972) The dosage-response curve for auxin-induced cell elongation: a reevaluation. Planta **104:** 1–9

**Cosgrove DJ** (2000) Loosening of plant cell walls by expansins. Nature **407:** 321–326

**Dharmasiri N, Dharmasiri S, Estelle M** (2005a) The F-box protein TIR1 is an auxin receptor. Nature **435:** 441–445

**Dharmasiri N, Dharmasiri S, Weijers D, Lechner E, Yamada M, Hobbie L, Ehrismann JS, Jürgens G, Estelle M** (2005b) Plant development is regulated by a family of auxin receptor F box proteins. Dev Cell **9:** 109–119

**Duby G, Boutry M** (2009) The plant plasma membrane proton pump ATPase: a highly regulated P-type ATPase with multiple physiological roles. Pflugers Arch **457:** 645–655

**Edelmann H, Schopfer P** (1989) Role of protein and RNA synthesis in the initiation of auxin-mediated growth in coleoptiles of *Zea mays* L. Planta **179:** 475–485

**Evans ML** (1974) Rapid responses to plant hormones. Annu Rev Plant Physiol **25:** 195–223

**Foissner I, Grolig F, Obermeyer G** (2002) Reversible protein phosphorylation regulates the dynamic organization of the pollen tube cytoskeleton: effects of calyculin A and okadaic acid. Protoplasma **220:** 1–15

**Frías I, Caldeira MT, Pérez-Castiñeira JR, Navarro-Aviñó JP, Culiañez-Maciá FA, Kuppinger O, Stransky H, Pagés M, Hager A, Serrano R** (1996) A major isoform of the maize plasma membrane $H^+$-ATPase: characterization and induction by auxin in coleoptiles. Plant Cell **8:** 1533–1544

**Fuglsang AT, Guo Y, Cuin TA, Qiu QS, Song CP, Kristiansen KA, Bych K, Schulz A, Shabala S, Schumaker KS, et al** (2007) *Arabidopsis* protein kinase PKS5 inhibits the plasma membrane $H^+$-ATPase by preventing interaction with 14-3-3 protein. Plant Cell **19:** 1617–1634

**Fuglsang AT, Visconti S, Drumm K, Jahn T, Stensballe A, Mattei B, Jenseni ON, Aducci P, Palmgren MG** (1999) Binding of 14-3-3 protein to the plasma membrane $H^+$-ATPase AHA2 involves the three C-terminal residues $Tyr^{946}$-Thr-Val and requires phosphorylation of $Thr^{947}$. J Biol Chem **51:** 36774–36780

**Gendreau E, Traas J, Desnos T, Grandjean O, Caboche M, Höfte H** (1997) Cellular basis of hypocotyl growth in *Arabidopsis thaliana*. Plant Physiol **114:** 295–305

**Hager A** (2003) Role of the plasma membrane $H^+$-ATPase in auxin-induced elongation growth: historical and new aspects. J Plant Res **116:** 483–505

**Hager A, Debus G, Edel H-G, Stransky H, Serrano R** (1991) Auxin induces exocytosis and the rapid synthesis of a high-turnover pool of plasma-membrane $H^+$-ATPase. Planta **185:** 527–537

**Hager A, Menzel H, Krauss A** (1971) Versuche und Hypothese zur Primärwirkung des Auxins beim Streckungswachtum. Planta **100:** 47–75

**Hayashi K, Neve J, Hirose M, Kuboki A, Shimada Y, Kepinski S, Nozaki H** (2012) Rational design of an auxin antagonist of the $SCF^{TIR1}$ auxin receptor complex. ACS Chem Biol **7:** 590–598

**Hayashi K, Tan X, Zheng N, Hatate T, Kimura Y, Kepinski S, Nozaki H** (2008) Small-molecule agonists and antagonists of F-box protein-substrate interactions in auxin perception and signaling. Proc Natl Acad Sci USA **105:** 5632–5637

**Hayashi M, Inoue S, Takahashi K, Kinoshita T** (2011) Immunohistochemical detection of blue light-induced phosphorylation of the plasma membrane $H^+$-ATPase in stomatal guard cells. Plant Cell Physiol **52:** 1238–1248

**Hayashi Y, Nakamura S, Takemiya A, Takahashi Y, Shimazaki K, Kinoshita T** (2010) Biochemical characterization of in vitro phosphorylation and dephosphorylation of the plasma membrane $H^+$-ATPase. Plant Cell Physiol **51:** 1186–1196

**Hertel R, Thomson KS, Russo VEA** (1972) In-vitro auxin binding to particulate cell fractions from corn coleoptiles. Planta **107:** 325–340

**Hörmanseder K, Obermeyer G, Foissner I** (2005) Disturbance of endomembrane trafficking by brefeldin A and calyculin A reorganizes the actin cytoskeleton of Lilium longiflorum pollen tubes. Protoplasma **227:** 25–36

**Inoue S, Kinoshita T, Shimazaki K** (2005) Possible involvement of phototropins in leaf movement of kidney bean in response to blue light. Plant Physiol **138:** 1994–2004

**Ishihara H, Martin BL, Brautigan DL, Karaki H, Ozaki H, Kato Y, Fusetani N, Watabe S, Hashimoto K, Uemura D, et al** (1989) Calyculin A and okadaic acid: inhibitors of protein phosphatase activity. Biochem Biophys Res Commun **159:** 871–877

**Jahn T, Johansson F, Lüthen H, Volkmann D, Larsson C** (1996) Reinvestigation of auxin and fusicoccin stimulation of the plasma-membrane $H^+$-ATPase activity. Planta **199:** 359–365

**Katou K, Okamoto H** (1992) Symplast as a functional unit in plant growth. Int Rev Cytol **142:** 263–304

**Kepinski S, Leyser O** (2005) The *Arabidopsis* F-box protein TIR1 is an auxin receptor. Nature **435:** 446–451

**Kerkeb L, Venema K, Donaire JP, Rodríguez-Rosales MP** (2002) Enhanced $H^+$/ATP coupling ratio of $H^+$-ATPase and increased 14-3-3 protein content in plasma membrane of tomato cells upon osmotic shock. Physiol Plant **116:** 37–41

**Kim Y-S, Min J-K, Kim D, Jung J** (2001) A soluble auxin-binding protein, ABP57: purification with anti-bovine serum albumin antibody and characterization of its mechanistic role in the auxin effect on plant plasma membrane $H^+$-ATPase. J Biol Chem **276:** 10730–10736

**Kinoshita T, Hayashi Y** (2011) New insights into the regulation of stomatal opening by blue light and plasma membrane $H^+$-ATPase. Int Rev Cell Mol Biol **289:** 89–115

**Kinoshita T, Shimazaki K** (1997) Involvement of calyculin A- and okadaic acid-sensitive protein phosphatase in the blue light response of stomatal guard cells. Plant Cell Physiol **38:** 1281–1285

**Kinoshita T, Shimazaki K** (1999) Blue light activates the plasma membrane $H^+$-ATPase by phosphorylation of the C-terminus in stomatal guard cells. EMBO J **18:** 5548–5558

**Kinoshita T, Shimazaki K** (2001) Analysis of the phosphorylation level in guard-cell plasma membrane $H^+$-ATPase in response to fusicoccin. Plant Cell Physiol **42:** 424–432

**Lee K, Kim M-I, Kwon Y-J, Kim M, Kim Y-S, Kim D** (2009) Cloning and characterization of a gene encoding $ABP_{57}$, a soluble auxin-binding protein. Plant Biotechnol Rep **3:** 293–299

**Lincoln C, Britton JH, Estelle M** (1990) Growth and development of the *axr1* mutants of *Arabidopsis*. Plant Cell **2:** 1071–1080

**Löbler M, Klämbt D** (1985) Auxin-binding protein from coleoptile membranes of corn (*Zea mays* L.). I. Purification by immunological methods and characterization. J Biol Chem **260:** 9848–9853

**Marre E** (1979) Fusicoccin: a tool in plant physiology. Annu Rev Plant Physiol **30:** 273–288

**Mockaitis K, Estelle M** (2008) Auxin receptors and plant development: a new signaling paradigm. Annu Rev Cell Dev Biol **24:** 55–80

**Moloney MM, Elliott MC, Cleland RE** (1981) Acid growth effects in maize roots: evidence for a link between auxin-economy and proton extrusion in the control of root growth. Planta **152:** 285–291

**Niittylä T, Fuglsang AT, Palmgren MG, Frommer WB, Schulze WX** (2007) Temporal analysis of sucrose-induced phosphorylation changes in plasma membrane proteins of *Arabidopsis*. Mol Cell Proteomics **6:** 1711–1726

**Paciorek T, Sauer M, Balla J, Wiśniewska J, Friml J** (2006) Immunocytochemical technique for protein localization in sections of plant tissues. Nat Protoc **1:** 104–107

**Paciorek T, Zazímalová E, Ruthardt N, Petrásek J, Stierhof Y-D, Kleine-Vehn J, Morris DA, Emans N, Jürgens G, Geldner N, et al** (2005) Auxin inhibits endocytosis and promotes its own efflux from cells. Nature **435:** 1251–1256

**Palmgren MG** (2001) Plant plasma membrane $H^+$-ATPases: powerhouses for nutrient uptake. Annu Rev Plant Physiol Plant Mol Biol **52:** 817–845

**Perrot-Rechenmann C** (2010) Cellular responses to auxin: division versus expansion. Cold Spring Harb Perspect Biol **2:** a001446

**Philippar K, Büchsenschütz K, Edwards D, Löffler J, Lüthen H, Kranz E, Edwards KJ, Hedrich R** (2006) The auxin-induced $K^+$ channel gene *Zmk1* in maize functions in coleoptile growth and is required for embryo development. Plant Mol Biol **61:** 757–768

**Philippar K, Ivashikina N, Ache P, Christian M, Lüthen H, Palme K, Hedrich R** (2004) Auxin activates *KAT1* and *KAT2*, two $K^+$-channel genes expressed in seedlings of *Arabidopsis thaliana*. Plant J **37:** 815–827

**Rayle DL, Cleland R** (1970) Enhancement of wall loosening and elongation by acid solutions. Plant Physiol **46:** 250–253

**Robert S, Kleine-Vehn J, Barbez E, Sauer M, Paciorek T, Baster P, Vanneste S, Zhang J, Simon S, Čovanová M, et al** (2010) ABP1 mediates auxin inhibition of clathrin-dependent endocytosis in *Arabidopsis*. Cell **143:** 111–121

**Rück A, Palme K, Venis MA, Napier RM, Felle HH** (1993) Patch-clamp analysis establishes a role for an auxin binding protein in the auxin stimulation of plasma membrane current in *Zea mays* protoplasts. Plant J **4:** 41–46

**Rudashevskaya EL, Ye J, Jensen ON, Fuglsang AT, Palmgren MG** (2012) Phosphosite mapping of P-type plasma membrane $H^+$-ATPase in homologous and heterologous environments. J Biol Chem **287:** 4904–4913

**Savaldi-Goldstein S, Baiga TJ, Pojer F, Dabi T, Butterfield C, Parry G, Santner A, Dharmasiri N, Tao Y, Estelle M, et al** (2008) New auxin analogs with growth-promoting effects in intact plants reveal a chemical strategy to improve hormone delivery. Proc Natl Acad Sci USA **105:** 15190–15195

**Schenck D, Christian M, Jones A, Lüthen H** (2010) Rapid auxin-induced cell expansion and gene expression: a four-decade-old question revisited. Plant Physiol **152:** 1183–1185

**Shinkle JR, Briggs WR** (1984) Auxin concentration/growth relationship for *Avena* coleoptile sections from seedlings grown in complete darkness. Plant Physiol **74:** 335–339

**Sondergaard TE, Schulz A, Palmgren MG** (2004) Energization of transport processes in plants: roles of the plasma membrane $H^+$-ATPase. Plant Physiol **136:** 2475–2482

**Svennelid F, Olsson A, Piotrowski M, Rosenquist M, Ottman C, Larsson C, Oecking C, Sommarin M** (1999) Phosphorylation of Thr-948 at the C terminus of the plasma membrane $H^+$-ATPase creates a binding site for the regulatory 14-3-3 protein. Plant Cell **11:** 2379–2391

**Teale WD, Paponov IA, Palme K** (2006) Auxin in action: signalling, transport and the control of plant growth and development. Nat Rev Mol Cell Biol **7:** 847–859

**Yamagami M, Haga K, Napier RM, Iino M** (2004) Two distinct signaling pathways participate in auxin-induced swelling of pea epidermal protoplasts. Plant Physiol **134:** 735–747